HYPODERMIC-NEEDLE-LIKE HOLLOW POLYMER MICRONEEDLE ARRAY USING UV LITHOGRAPHY INTO MICROMOLDS

Po-Chun Wang, Seung-Joon Paik, Jooncheol Kim, Seong-Hyok Kim, and Mark G. Allen
School of Electrical and Computer Engineering, Georgia Institute of Technology, Atlanta, Georgia, USA

ABSTRACT

This paper presents a polymer hollow microneedle array for transdermal drug delivery that is fabricated using UV photolithography and a single-step micromolding technique. This fabrication process patterns a 6×6 array of 1mm tall high-aspect-ratio hollow microneedles with sharp beveled tips and 150μm diameter side-opened lumens. The geometry of the beveled tip and the position of the lumen are defined simultaneously by a two-dimensional lithography mask pattern and the topography of the micromold. This three-dimensional geometry improves insertion performance and potentially the drug delivery efficiency without additional fabrication processes. These hypodermic-needle-like microneedles have been successfully constructed, packaged, and tested for fluidic functionality and skin penetrability.

INTRODUCTION

Hypodermic needles are widely used for drug and vaccine delivery. Their characteristic sharp beveled tips and large side openings allow ease of insertion and efficient, nearly clog-free drug delivery. The introduction of bevels to hypodermic needles thins the needle tips and reduces the required penetration force into skin as well as alleviates the pain perceived by patients during insertion [1, 2]. The side-opened lumens are expected to be less susceptible to tissue clogging during insertion and form a larger fluid up-take area in the skin [3-5]. Compared to microneedles with side openings, needles with top openings exhibited poor fluid delivery performance [3], suggesting the importance of the lumen opening location in the needle design to maximize its drug delivery capability. A recent study demonstrated that hollow microneedles with a beveled tip and side-opened lumen successfully delivered insulin to human patients with type 1 diabetes [6].

Several fabrication approaches have been reported to mimic the tip profile of hypodermic needles. Anisotropic etching of silicon produced sharp tips for microneedles with a fixed tip slope angle [7, 8], silicon dry etching followed by serial saw dicing produced beveled tips on high-aspect-ratio silicon tubes [9], and deep x-ray lithography combined with a two-step micromolding technique enabled fabrication of polymer microneedles with beveled tips and side openings [10]. In those approaches, sharp beveled tips were achieved at the expense of the involvement of multiple complex process steps or facilities with limited availability.

In this paper, a simple combination of UV photolithography and single-step micromolding is proposed to fabricate an array of hypodermic-needle-like polymer microneedles with sharp beveled tips and large side-openings for drug delivery.

DESIGN

Figure 1 illustrates the key fabrication concept for the proposed microneedle fabrication. In Figure 1(a), a circular pattern on the mask is projected onto the slope of a mold, creating an elliptical shape. A variety of shapes on the mold can be achieved by altering the pattern on the mask. Figure 1(b) shows the use of UV light radiation with the mask pattern to define the beveled tip, lumen, and shaft of a hollow microneedle by cross-linking a negative photoresist, SU-8, between the mask and the mold. The bevel angle of the needle tip is defined by the angle of the slope on the mold, which can be modified during the construction of the mold. The key fabrication concept is to define the slope and shape of the beveled tip as well as the position of the lumen by a combination of the mold slope and photolithography. Therefore, the proposed process allows the geometry of the microneedle tip to be optimized three-dimensionally for ease of insertion and efficient drug delivery without additional fabrication processes. In addition, the proposed process eliminates the dependence of the tip sharpness on the bottom corner of the mold [11].

Figure 2 shows an optical image of a 26 gauge hypodermic needle and three-dimensional CAD drawings of microneedle tips obtainable from different mask designs. The angle of the mold slope is 35° in all three drawings in Figure 2(b).

FABRICATION

The fabrication process of the hollow microneedle array consists of two steps. The first step is to construct a reusable

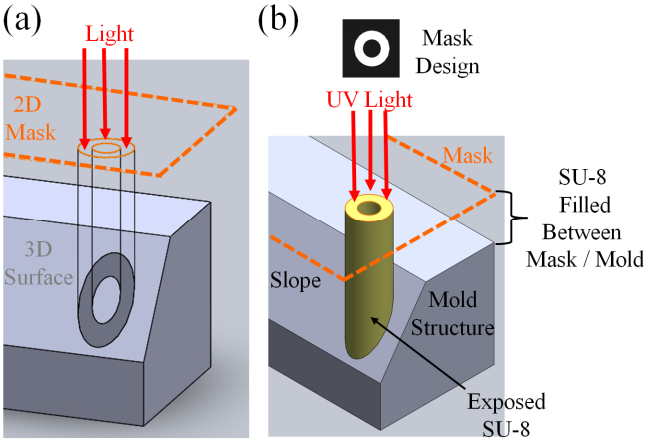

Figure 1: (a) A depiction showing the projection of a two-dimensional (2D) mask pattern onto a three-dimensional (3D) surface. (b) Illustration of the construction of a proposed microneedle structure by a combination of UV radiation and the topography of a mold.

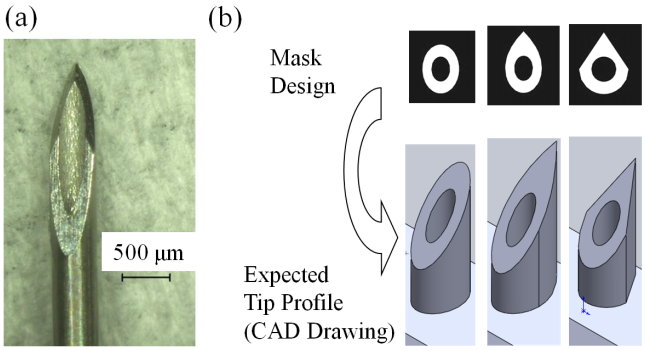

Figure 2: (a) Optical image of a 26 gauge hypodermic needle. (b) CAD drawings of three microneedle tips projected from different mask designs.

polydimethylsiloxane (PDMS) mold using the inclined photolithography process [12]. The second step is to fabricate the hollow SU-8 microneedle on the constructed PDMS mold. Figure 3 shows the fabrication process flow of the hollow microneedle on the PDMS mold. A quantity of SU-8 2025 resist was first preheated at 60°C for 30 minutes in order to ultimately improve its penetration of the micro-trenches in the PDMS mold. The PDMS mold was treated using oxygen plasma for 20 minutes to increase the PDMS surface energy prior to the SU-8 encapsulation (Figure 3(a)). The preheated SU-8 was then cast by weight onto the PDMS mold to obtain a thickness of 600µm. A one-hour backside vacuuming process was performed to eliminate the bubbles trapped in the PDMS trenches (Figure 3(b)). The SU-8/PDMS sample was then soft baked at 85°C for 16 hours on a hotplate.

UV (365nm, I-line) light was used to define the hollow microneedle structure. The photolithography process consists of two exposure steps with separate masks. In the first exposure step, the beveled tip, lumen, and shaft of a hollow microneedle were defined (Figure 3(c)) with a UV dosage of 1800 mJ/cm^2. A post-exposure-bake (PEB) was then carried out on a hotplate at 85°C for 30 minutes. In the second exposure step, the baseplate of the microneedle array was defined using a mask that protected the needle lumens from exposure with a reduced UV dosage of 350 mJ/cm^2 (Figure 3(d)). The second PEB process was performed in an oven at 85°C for 15 minutes.

The SU-8 layer was then demolded from the PDMS mold and immersed into a propylene glycol methyl ether acetate (PGMEA) bath for six hours without stirring to develop the SU-8 (Figure 3(e)). The sample was rinsed with isopropyl alcohol (IPA) solution and blown dry. The completed SU-8 hollow microneedle structure is shown in Figure 3(f). Prior to the skin insertion test, the fabricated microneedle array was treated by flood UV exposure on both sides and then hard baked at 135°C for 30 minutes on a hot plate.

Figure 4 shows three different mask designs and corresponding fabricated hollow microneedles. A variety of tip geometries can be fabricated with different mask designs. The hollow microneedle shown in Figure 4(c) is 980µm tall with a base width of 300µm. The spacing between the lumen opening and the base plate is 590µm.

CHARACTERIZATION

The fluidic functionality of the fabricated hollow microneedle array was characterized, as shown in Figure 5, using the custom package and fluid test setup in [11]. The microfluidic characterization, which utilized a dye-filled syringe, indicated that at least 85% of the lumens were open, and the total fluidic flow rate was 2 ml/min.

The skin penetrability of the fabricated hollow microneedle shown in Figure 4(c) was evaluated with excised porcine skin. The excised porcine skin (Pel-Freez, Rogers, AR) was shaved using a razor, followed by the removal of the subcutaneous fat with a scalpel. The prepared skin was then affixed under mild tension to a wooden block using screws. The baseplate of the microneedle array was attached to a scanning-electron-microscope (SEM) mount using a double-sided tape. The needle array was then pressed against the porcine skin by thumb or an automatic insertion test machine, followed by separation of the array from the

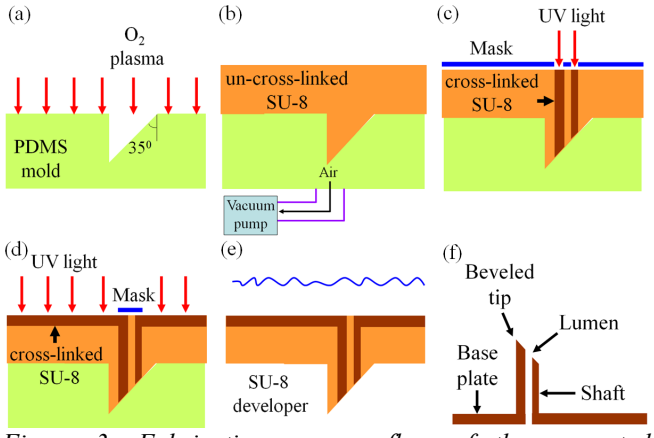

Figure 3: Fabrication process flow of the presented microneedle structures. The exposure energy in step (c) is 1800 mJ/cm^2, and that in step (d) is 350 mJ/cm^2.

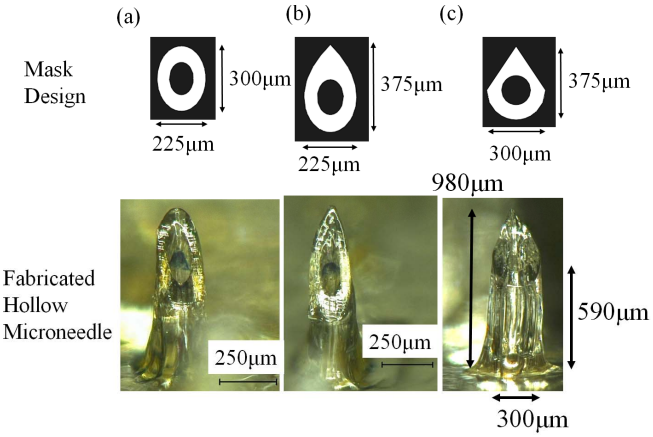

Figure 4: Three different mask designs and optical micrographs of corresponding fabricated hollow microneedles.

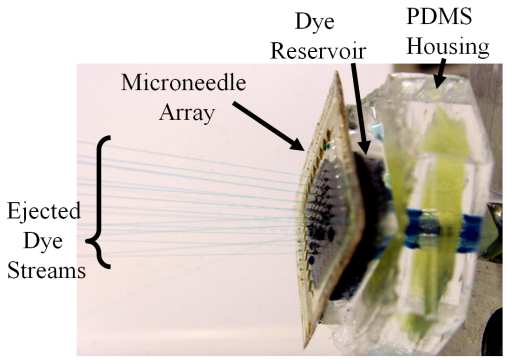

Figure 5: Optical still image of the packaged hollow microneedle array in a microfluidic test. Eighteen visible streams ejected from an array of 21 hollow microneedles, suggesting an open lumen yield of 85%.

skin. One drop of blue dye was then dispensed onto the skin surface. The dye flowed through the microneedle-defined pathways in the stratum corneum (SC) and stained the viable epidermis underneath. Stain in the viable epidermis serves as an indication of successful insertion of the microneedle into the skin. The skin surface was then wiped with alcohol swabs to remove the residual dye on the skin, followed by inspection of the skin under an optical microscope.

Figure 6(a) shows successful manual insertion of the 6×6 microneedle array into the skin. Following the insertion, thirty-five pathways were easily identified under an optical microscope. Thirty-five successful insertion holes out of the fabricated 6×6 needle array suggested a manual insertion yield of 97%. The failed insertion point corresponds to a broken tip of the microneedle observed prior to the insertion test. Figure 6(b) shows a close-up view of an insertion site, where the red triangle at the center indicates the pathway created by insertion and the black circle highlights the region where the dye diffused underneath the stratum corneum through the pathway. Figures 6(c) and 6(d) show the side-views of the same microneedle prior to and following insertion, respectively. There is no visible damage to the microneedle after the insertion.

Figure 7 shows a preliminary comparison of insertion performance between the pyramidal-tip microneedle [11] and this proposed hypodermic-needle-like microneedle. An automatic insertion test machine with a controlled slow driving rate of 1.2 mm/sec was used for the test to ensure that the two needle arrays were pressed against the skin with identical forces of 35N. The insertion fidelity of the beveled-tip microneedle array resulting from slow machine insertion was ~44%, which is significantly higher than that of the previous pyramidal-tip array (~11%). The superior insertion performance of the fabricated beveled-tip microneedle over its pyramidal-tip counterpart was not attributed to the tip sharpness, since both needles showed similar tip diameters (not shown). The beveled-tip design exhibited a higher aspect ratio on the tip end by thinning the tip structure, and a thinner tip profile is reported to lower the penetration force into skin in a study of hypodermic needles [1].

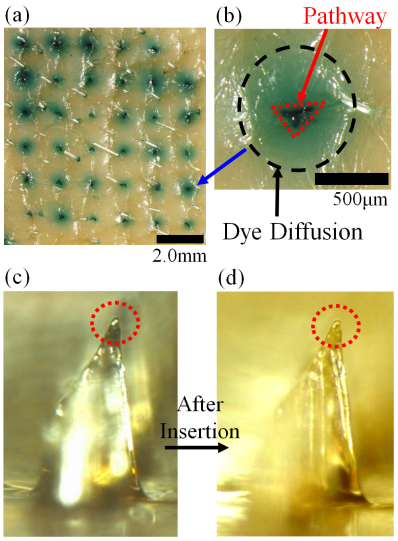

Figure 6: (a) Optical micrograph of the excised porcine skin following the manual insertion of a 6×6 microneedle array. (b) A close-up view of an insertion site, showing the pathway created by microneedle insertion and the subsequent dye diffusion underneath the stratum corneum. (c)(d) Optical micrographs of the side-view of the same microneedle prior to and following manual insertion into excised porcine skin, respectively. The dashed red circles indicate the locations of microneedle tips.

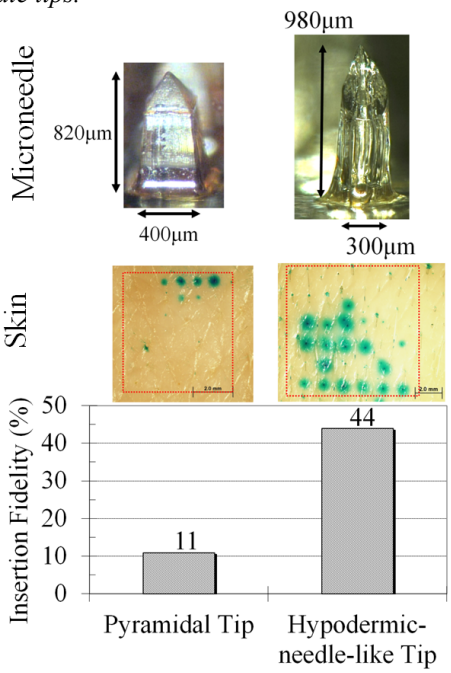

Figure 7: A comparison chart of insertion performance between the pyramidal tip and hypodermic-needle-like tip. Both arrays are in a 6×6 configuration. The two upper figures show optical images of pyramidal and hypodermic-needle-like tips, and the two center figures are the corresponding optical images of the porcine skin following insertion. The 16 insertion pathways created by the 6×6 microneedle array of hypodermic-needle-like tip corresponds to an insertion fidelity of 44%.

CONCLUSION

A hypodermic-needle-like hollow polymer microneedle array for transdermal drug delivery is fabricated using UV lithography and a single-step micromolding process. This 6×6 array consists of 1mm tall high-aspect-ratio SU-8 hollow microneedles with sharp beveled tips and 150μm diameter side-opened lumens. The geometry of the beveled tip and the position of the lumen are defined by a two-dimensional mask pattern in photolithography and the topography of the micromold, and optimized for easy insertion. The needle array was packaged and characterized for fluidic functionality and skin penetrability. The fluid characterization indicated that at least 85% of the lumens were open and the total fluidic flow rate was 2 ml/min. A manual insertion test with excised porcine skin showed a successful insertion rate of 97% and no visible damage to the microneedles following insertion. In addition, the hypodermic-needle-like microneedles exhibited superior insertion performance over microneedles with a pyramidal tip.

ACKNOWLEDGEMENT

The authors would like to thank Dr. Jeong-Woo Lee in the Laboratory for Drug Delivery at the Georgia Institute of Technology for his help on the automatic insertion test station. This project is supported by National Institutes of Health under grant numbers of R01-EB006369 and 1U01AI074579.

REFERENCES

[1] L. Vedrine, W. Prais, P. E. Laurent, C. Raynal-Olive, and M. Fantino, "Improving needle-point sharpness in prefillable syringes", *Med. Device Technol.*, vol. 14, pp32-35, 2003.

[2] A. Jaber, G. B. Bozzato, L. Vedrine, W. A. Prais, J. Berube, and P. E. Laurent, "novel needle for subcutaneous injection of interferon beta-1a: effect on pain in volunteers and satisfaction in patients with multiple sclerosis", *BMC Neurology*, vol. 8, article no. 38, 2008.

[3] R. K. Sivamani, B. Stoeber, G. C. Wu, H. B. Zhai, D. Liepmann, and H. Maibach, "Clinical microneedle injection of methyl nicotinate: stratum corneum penetration", *Skin Research and Technology*., vol. 11, pp. 152-156, 2005.

[4] T. Frisk, N. Roxhed, and G. Stemme, "MEMS for medical technology applications", in *Proc. SPIE*, vol. 6465, pp646513-1-9, 2007.

[5] P. Zhang, C. Dalton, and G. A. Jullien, "Design and fabrication of MEMS-based microneedle arrays for medical applications", *Microsys. Techno.*, vol. 15, pp1073-1082, 2009.

[6] J. Gupta, E. I. Felner, M. R. Prausnitz, "Minimally Invasive Insulin Delivery in Subjects with Type 1 Diabetes Using Hollow Microneedles", *Diabetes Technol. Ther.*, vol. 11, pp. 329-337, 2009.

[7] H. J. G. E. Gardeniers, R. Luttge, E. J. W. Berenschot, M. J. de Boer, S. Y. Yeshurun, M. Hefetz, R. Van't Oever, A. van den Berg, "Silicon micromachined hollow microneedles for transdermal liquid transport", *J. Microelectromech. Syst.*, vol. 12, pp. 855-862, 2003.

[8] R. Luttge, E. J. W. Berenschot, M. J. de Boer, D. M. Altpeter, E. X. Vrouwe, A. van den Berg, M. Elwenspoek, "Integrated lithographic molding for microneedle-based devices", *J. Microelectromech. Syst.*, vol. 16, pp. 872-884, 2007.

[9] N. Baron, J. Passave, B. Guichardaz, G. Cabodevila, "Investigations of development process of high hollow beveled microneedles using a combination of ICP RIE and dicing saw", *Microsyst. Technol.*, vol. 14, pp. 1475-1480, 2008.

[10] M. Matteucci, M. Fanetti, M. Casella, F. Gramatica, L. Gavioli, M. Tormen, G. Grenci, F. De Angelis, E. Di Fabrizio, "Poly vinyl alcohol re-usable masters for microneedle replication", *Microelectronic Eng.*, vol. 86, pp. 752-756, 2009.

[11] P. Wang, B. A. Wester, S. Rajaraman, S. Paik, S. Kim, M. G. Allen, "Hollow polymer microneedle array fabricated by photolithography process combined with micro- molding techniques", in *Proc. IEEE EMBC 2009*, Minneapolis, Sept. 2-6, 2009, pp. 7026-7029.

[12] S. Rajaraman, M. A. McClain, S. Choi, J. D. Ross, S. P. Deweerth, M. C. LaPlaca, M. G. Allen, "Three-dimensional metal transfer micromolded microelectrode arrays (MEAs) for in-vitro brain slice recordings", in *Proc. Transducers 2007*, Lyon, France, June 10-14, 2007, pp. 1251-1254.